AIAA JOURNAL
Vol. 31, No. 2, February 1993

Visualization of the Flows in Precessing Tanks with Internal Baffles

Richard Manasseh*
University of Cambridge, Cambridge, England, United Kingdom

This paper presents an experimental investigation of some fluid flows inside a precessing right circular cylindrical tank. The first aim was to determine the extent to which a wave modal description of the fluid flow, which is physically realizable for a tank with no internal baffles, is sustained when the geometry of the tank is modified by baffle plates. The second was to determine if a baffle plate configuration could be found that forestalled the development of low-order modes. This second aim is directed toward the goal of eliminating low-order mode resonances in the fuel tanks of spinning spacecraft. Instabilities of such spacecraft have been successfully minimized at the design stage by the incorporation of baffle plates optimized by empirical "drop tests." The ability of a baffle plate to eliminate low-order resonances, provided it is of a particular optimal configuration, is confirmed in this paper. This result suggests the use of flow visualizations as a means of simplifying expensive empirical drop-test programs.

I. Introduction

IN recent years, increasing proportions of the masses of spacecraft have been made up of fluids. These are the liquid fuels required to make small corrections to the orbits of communications satellites that are becoming more complex and must stay in operation for longer times. Spinning interplanetary probes must also carry more liquid fuels to execute increasingly complex missions. The stability of such spacecraft must be insured at the design stage.

A rigid spacecraft will spin stably about either its axis of least inertia or its axis of greatest inertia. However, if energy is dissipated when a spacecraft is spinning about its axis of least inertia (a common configuration for a satellite in geostationary transfer orbit), this configuration is unstable. The spacecraft's nutation angle diverges as it tends to a spin about its axis of greatest inertia, this being the state of lowest energy for a given angular momentum.

In a spacecraft containing liquid fuels, "dissipation" can include the transfer of energy from the rigid spacecraft's motion to the fluid. The fluid motion could occur on a variety of spatial scales, ranging from the large (low wave number waves) to the small (turbulence). In addition, viscous friction causes energy losses in boundary or shear layers.

Drop-test experiments[1] were carried out on scaled models of the Eurostar spacecraft bus. The internal liquid-containing tanks in both the models and the prototype spacecraft were right circular cylinders with hemispherical ends. In a drop-test experiment, a scale model of the spacecraft and its contained fluids is spun up at the top of a shaft. The model is dropped and briefly experiences free fall. During its fall, the model's overall angular velocity is recorded so that the prototype's stability in orbit may be inferred. Exponential growth of the nutation angle θ of the spinning model was reported; the model was unstable. The nutation angle diverged according to $\theta \propto e^{t/\tau}$, with experimental time constants τ of order 1 s. This occurred even with virtually full fuel tanks. Corresponding scaled time constants for the prototype spacecraft of about 20–30 s (or 10–15 revolutions of the spacecraft) were unacceptably short. Tests with a "dry" system, for which Euler's equations of rigid-body dynamics predict stability, confirmed that the instability was due to the presence of fluids on board the spacecraft.

The characteristic fluid time scale associated with viscosity is $(R\Omega^{1/2})/\nu^{1/2}$, where R is a length scale, Ω the rotation rate, and ν the kinematic viscosity.[2] If we only admit the possibility of dissipation in the spacecraft due to boundary or shear layer friction (rather than waves or turbulence), that implies a transfer from the kinetic energy of the spacecraft's rotation to the fluid, on a time scale of a few hundred seconds. Thus it seems probable that the drop-test time constants of order tens of seconds[1] are due to more rapid effects in the fluid than those caused by viscous diffusion alone.

The drop-test program described by Pocha[1] was conducted to determine empirically how best to increase τ, without any attempt to understand the fluid dynamics involved. The tests involved fitting various baffle plates in the tank and conducting an exhaustive series of tests to determine the baffle configuration that maximized τ. This program was successful. The optimum baffle plate was found to be one normal to the tank axis, with a central hole of radius r. The optimum ratio of r to the tank radius R was found to be 0.5. The Eurostar satellite bus was designed on this basis, and several versions of it are currently performing their roles in orbit. However, the expense of empirical drop-testing is an impediment in the design of future spin-stabilized spacecraft. Other experimental systems exist, for example, air-bearing supported rigs and those incorporating measurements of the energy dissipated. They, too, support mainly empirical studies, which do not investigate the actual fluid motion.

This paper describes some work conducted as part of a project aimed at improving the understanding of the fundamental fluid dynamics involved in the more rapid instabilities reported by Pocha.[1] (The project work was done at the Department of Applied Mathematics and Theoretical Physics, University of Cambridge, England.) The system analyzed in this paper is one stage removed from the real engineering problem, in which there is a mutual interaction of the rigid spacecraft and its contained fluids. In this paper the fluid response to a prescribed rigid-body forcing is considered. It is hoped that a detailed investigation of the fluid response will aid the prediction and prevention of the processes that lead to a loss of stability of the coupled spacecraft-fluid system. The system is further simplified by considering the tank geometry to be a right circular cylinder with planar rather than hemispherical ends.

Received Nov. 19, 1991; revision received June 25, 1992; accepted for publication June 30, 1992.

*Research Assistant, Department of Applied Mathematics and Theoretical Physics; currently, Research Associate, School of Mathematics, University of New South Wales, P.O. Box 1, Kensington, NSW 2033, Australia.

A detailed investigation of the fluid response should begin with a description of the inertia waves that can occur in a spinning tank. These waves, which can arise in a completely filled tank, are made possible by the Coriolis force that exists in a spinning system.

II. Formulation

Referring to Fig. 1, consider a general fluid-filled container spinning about an axis through its centroid and precessing about a second axis through its centroid. Assume the centroid is not accelerating in inertial space and the angle between the two axes is not varying with time. In rotating fluid dynamics problems one typically chooses the basic rotation period of the fluid relative to inertial space as the time scale; in our problem this is $\Omega^{-1} = |(\omega_1\hat{k} + \omega_2\hat{K})|^{-1}$. Here, however, we will choose the time scale to be ω_1^{-1}. In making this choice of time scale, we are anticipating observing experiments from a frame of reference in which periods of $2\pi/\omega_1$ are easily counted to provide a time scale with which various events can be measured. In fact, in the experiments to be described later, ω_1^{-1} is the rotation period of the tank relative to the observing cameras. The length scale R is equal to the container radius. The cylinder length/radius aspect ratio is h. Assume that the nutation angle θ between the two axes is small and that the velocity scale $U = \mathcal{O}(\omega_1 R\theta)$ allows linearization of the problem. The dimensional pressure is $\rho\omega_1 URp$, where p is the dynamic pressure in excess of the centrifugal pressure that plays no dynamical role in this problem, since the container is completely filled. The nondimensional excitation frequency ω is defined as twice the ratio of the basic rotation rate Ω to first order in θ, to the frequency of the variation of the overall angular velocity vector in tank coordinates ω_1, giving $\omega = 2[1 + (\omega_2/\omega_1)]$.

The incompressible inviscid linearized fluid equation of motion relative to axes fixed in the container is

$$\frac{\partial \boldsymbol{u}}{\partial t} + \omega\hat{k} \times \boldsymbol{u} + \nabla p = -(\omega - 2)[r\cos(\phi + t)]\hat{k} \tag{1}$$

together with continuity,

$$\nabla \cdot \boldsymbol{u} = 0 \tag{2}$$

Equation (1) is the form of the momentum equation appropriate to our problem; steps in its derivation are outlined by Wood.[3] Its homogeneous form expresses the balance between inertia, Coriolis, and pressure gradient forces. The inhomogeneous term on the right-hand side comes from the variation of the overall angular velocity vector with time, due to the precession imposed on the container. This is the forcing applied to the system. The boundary condition is

$$\boldsymbol{u} \cdot \hat{\boldsymbol{n}} = 0 \tag{3}$$

where $\hat{n}$ is the unit normal vector to the container surface. This allows a free-slip condition at the container wall consistent with our assumption of an inviscid flow. To effect the inviscid approximation, the Ekman number, defined by $E = \nu/(\omega_1 R^2)$, has been assumed to be negligibly small.

To find the set of steady-state wave modes in a cylindrical tank, seek a complementary function to Eq. (1) satisfying the boundary conditions. Adopt cylindrical polar coordinates (r, ϕ, z) fixed in the tank, with their origin at the cylinder centroid. Assuming a separable solution of form

$$\boldsymbol{u} = \sum_{n=1}^{\infty} \boldsymbol{U}_n e^{it} \tag{4}$$

$$p = \sum_{n=1}^{\infty} Q_n(r, \phi, z)e^{it} \tag{5}$$

and eliminating the velocity components with the aid of the continuity equation, gives Poincaré's equation,

$$\frac{1}{r}\frac{\partial}{\partial r}\left(r\frac{\partial Q_n}{\partial r}\right) + \frac{1}{r^2}\frac{\partial^2 Q_n}{\partial \phi^2} + (1 - \omega^2)\frac{\partial^2 Q_n}{\partial z^2} = 0 \tag{6}$$

a hyperbolic partial differential equation (PDE) for $|\omega| > 1$. The associated boundary condition is

$$\boldsymbol{U} \cdot \hat{\boldsymbol{n}} = 0 \tag{7}$$

which can be expressed in terms of the pressure amplitude as

$$i\frac{\partial Q_n}{\partial r} + \omega\frac{1}{r}\frac{\partial Q_n}{\partial \phi} = 0, \qquad r = 1 \tag{8}$$

$$\frac{\partial Q_n}{\partial z} = 0, \qquad z = \pm h/2 \tag{9}$$

In an unbounded domain Eq. (6) admits a set of plane-wave solutions that are usually referred to in the literature as inertia waves. Although the full problem given by Eqs. (6) and (7) is ill posed, it is possible to find an analytic description of the flow in the case of the particular geometry of a right circular cylinder.

For brevity, the index n is used to indicate a unique combination of the spatial wave numbers k, λ, and m. The integer k is the axial wave number and the integer m is the azimuthal wave number. As the radial wave number λ is noninteger, it is convenient to use an integer index l to count the number of half-cycles in the radial direction. The wave number vector is then $\{k, l, m\}^T$.

A solution to Eqs. (6) and (7) by separation of variables is

$$Q_n = J_m(\lambda_n r)\cos[(\omega^2 - 1)^{-1/2}\lambda_n(z + h/2)]e^{im\phi} \tag{10}$$

where J_m is the Bessel function of the first kind, order m. A solution to Poincaré's equation of this kind was first found by Kelvin.[4]

The modes arising from precessional forcing have azimuthal wave number $m = 1$ [since the forcing term on the right-hand side of Eq. (1) goes as $\cos(\phi + t)$], so the radial wave numbers are given by the roots of

$$\lambda\frac{\partial J_1(\lambda)}{\partial r} + \omega J_1(\lambda) = 0 \tag{11}$$

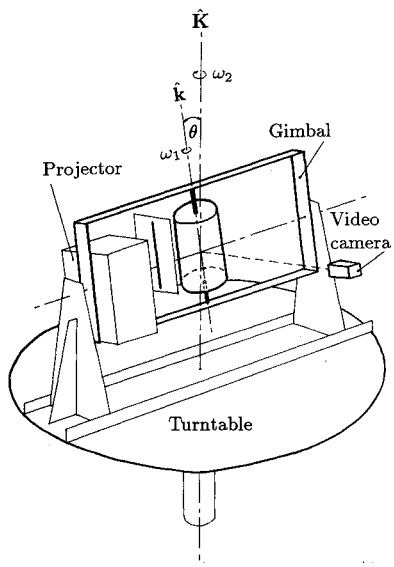

Fig. 1 Schematic diagram of the apparatus. Unit vector $\hat{k}$ fixed in spinning tank; unit vector $\hat{K}$ fixed in turntable. Video camera fixed in turntable frame; its line of sight is normal to $\hat{k}$.

Table 1 Resonant excitation frequencies ω_{klm} and radial wave numbers λ_{klm} for a precessionally forced cylinder, $h = 8/3$

k	l	ω_{kl1}	λ_{kl1}	k	l	ω_{kl1}	λ_{kl1}
1	1	2.64298	2.88221	4	1	1.12769	2.45622
1	2	5.27757	6.10489	4	2	1.55603	5.61787
1	3	7.93621	9.27678	4	3	2.11440	8.77909
2	1	1.48403	2.58361	5	1	1.08229	2.43833
2	2	2.65374	5.79180	5	2	1.37830	5.58728
2	3	3.93395	8.96479	5	3	1.78975	8.74335
3	1	1.22370	2.49274	6	1	1.05736	2.42833
3	2	1.89134	5.67380	6	2	1.27306	5.56886
3	3	2.69398	8.84105	6	3	1.58812	8.72081

to satisfy the radial boundary condition (8). To satisfy the axial boundary condition (9) with integer k,

$$\omega^2 = 1 + \left(\frac{\lambda_{kl1} h}{k\pi}\right)^2 \tag{12}$$

where λ_{kl1} is the lth root of Eq. (11). Resonant excitation frequencies are thus values of ω satisfying Eqs. (11) and (12). Some of the lower order ω_n are given (Table 1) for the cylinder length/radius ratio h of the experiment in this study.

Note that the ω_n do not increase monotonically with increasing order of the wave number vector. The ω_n are densely spaced; for any ω_n, it is possible to find another arbitrarily close. For ω to be close to an ω_n such that $\omega_n < 2.0$, $\mathrm{sgn}(\omega_2) = -\mathrm{sgn}(\omega_1)$, i.e., the sense of precession is retrograde, opposite to the sense of spin. However, although the precession becomes retrograde as the frequency passes from $\omega = 2^+$ to 2^-, the waves are still traveling in the same sense, in tank coordinates. Opposite-traveling waves will not be forced until $\omega < -1$. In the spacecraft context, the precession must be prograde, in the same sense as the spin, to represent the motion of a typical vehicle that is "inertially prolate." The lowest order mode in Table 1, which is studied in these experiments, occurs in prograde precession.

The velocity field $\boldsymbol{u} = Re\Sigma_{n=1}^{\infty}(A_n U_n e^{it})$ found by using Eq. (1) and the solution (10) is given by

$$\boldsymbol{u} = \sum_{n=1}^{\infty} A_n \begin{Bmatrix} -\dfrac{1}{1-\omega_n^2}\left[\dfrac{dJ_1(\lambda_n r)}{dr} + \omega_n \dfrac{1}{r} J_1(\lambda_n r)\right] \\ \cdot \cos[k\pi(z/h + \tfrac{1}{2})]\sin(\phi + t) \\ \dfrac{-1}{1-\omega_n^2}\left[\omega_n \dfrac{dJ_1(\lambda_n r)}{dr} + \dfrac{1}{r} J_1(\lambda_n r)\right] \\ \cdot \cos[k\pi(z/h + \tfrac{1}{2})]\cos(\phi + t) \\ \dfrac{k\pi}{h} J_1(\lambda_n r)\sin[k\pi(z/h + \tfrac{1}{2})]\sin(\phi + t) \end{Bmatrix} \tag{13}$$

and the pressure by

$$p = \sum_{n=1}^{\infty} \frac{\omega}{\omega_n} A_n J_1(\lambda_n r)\cos[k\pi(z/h + \tfrac{1}{2})]\cos(\phi + t) \tag{14}$$

[The amplitudes A_n are found by calculating the inner-product integral of the forcing function that is on the right-hand side of Eq. (1), using the spatial structure of the nth mode. The amplitudes are not required for the purposes of this paper.]

Wood[3] has shown that the linear inviscid solution in a cylindrical tank is a true approximation to a linear viscous solution as the inviscid limit ($E = 0$) is approached. However, his solution exhibits discontinuities in velocity gradient on singular surfaces. These surfaces are cones with half-angle $\alpha = \tan^{-1}(\omega^2 - 1)^{-1/2}$; effectively the characteristics of the hyperbolic PDE (6). The velocity gradient discontinuities were interpreted as locally large shears on the singular surfaces, the shear being small elsewhere in the body of the fluid. It is interesting to know the characteristic angle α, as it is the angle at which energy propagates at the group velocity for inertia waves. In adopting a linear inviscid solution, it should be remembered that nonlinear effects, such as mode interactions and flow breakdowns, cannot be predicted.

In principle all of the linear inviscid modes could be forced, up to the order where the wavelength is comparable to the boundary-layer thickness. However, the modes that can be precessionally forced have $m = 1$, as noted earlier. Furthermore, the forcing function $-(\omega - 2)[r\cos(\phi + t)]\hat{k}$ is even in z, so that the modes on which it will project must have a vertical velocity that is also even in z, requiring, from Eq. (13), an odd axial wave number k. Low-order modes are those with a small wave number vector magnitude.

III. Geometric Modifications

A large-scale motion of the fluid is the most probable cause of the rapid instability described by Pocha,[1] which can occur with virtually full tanks. In this scenario, wave modes resonate in the tanks in response to a small coning motion of the spacecraft. This rapidly transfers energy from the rotation of the spacecraft to internal fluid motion. If this is the case, the optimum baffle configuration found by Pocha[1] is that for which modal resonances are avoided.

As noted in Sec. II, the eigenmode problem in the case of contained inertia waves is ill posed. That is, it requires the solution of a hyperbolic PDE with boundary conditions normally associated with elliptic equations. Consequently, it is suspected that the physical realization of "modes" may be very sensitive to changes in the internal geometry. To generate a mode structure, energy propagating from the tank walls at the group velocity for inertia waves takes a finite time to retrace its path in the tank.

Thus, even if modes are predicted, under linear theory, to develop in a modified geometry, more rapid effects (such as spatial or temporal interactions with other waves) may preclude the development of a simple mode structure. Indeed, there is evidence that the fluid generally breaks down to nonlinear behavior. In a study of the fluid motion inside a liquid-filled gyroscope, Scott[5] noted the periodic appearance and demise of a free-surface wave form that was not predicted by linear inviscid theory. Whiting[6] made pressure measurements in a system kinematically identical to the one described in this paper. He noted that at coning angles (θ in this paper) "as small as 5×10^{-4}, the data showed significant departure from the predictions of linear theory, and at coning angles as small as 8×10^{-4}, the liquid exhibited nonstationary behavior suggestive of a flow instability."

Several studies of rotating fluid systems (for example, Malkus,[7] McEwan,[8] Manasseh[9] and Manasseh[10]) have documented fluid flow breakdowns leading to turbulence. In Manasseh,[10] different breakdown regimes were cataloged by a letter scheme (A-G), where a type A breakdown results in the generation of turbulence with the smallest scales. Under the assumption that organized resonating flows lead to rapid instabilities of the spacecraft, a prompt transition to chaos would be desirable. Any resulting turbulence will result in substantial energy losses, of course, but over a longer time scale. This is because the disorganized turbulent fluid motion, once generated, would exert only a small average torque on the rigid spacecraft, compared with the large torque applied by an organized resonating mode.

There is, therefore, both scientific and engineering interest in exploring the behavior of the fluid in a container where the geometry has been modified.

The form of baffle found[1] to be most effective was a plate normal to the tank axis with a central hole of radius r. Naïvely, we might postulate that a modal description of the flow remains valid even under the modifications to the geometry introduced by such baffles. Then, for a baffle with a large hole, we would expect essentially the same fundamental mode to be observed when forced near resonance, as in the original

tank. With a small hole, the tank is effectively sectioned in two and we would expect that in each half the flow would adopt a modal structure appropriate to a tank of half the height; the eigenfrequencies for cylinders of the appropriate aspect ratios are given in Table 2 (which is specific to the Perspex baffle insert used in these experiments). An intermediate-sized hole could then be found for which neither modal solution is valid. This possibility is to be tested experimentally, by means of flow visualization.

Three baffles were chosen. The baffle with the intermediate-sized hole had an r/R ratio of 0.622. This was chosen so that there would be a sharp boundary at the point where, from Eq. (13), the maximum vertical flow velocities are expected for the (1, 1, 1) mode, i.e., at the first peak of a Bessel function $J_1(\lambda r)$, λ being the radial wave number for the (1, 1, 1) mode. This choice is naïve but is consistent with the assumption that the geometrical perturbation is an "obstacle" precluding the temporal development of the (1, 1, 1) mode. The baffle with the largest hole had an r/R of 0.777; the smallest had an r/R of 0.222. These were chosen to give an r/R ratio well above and below that of the intermediate baffle, under the practical constraints governing the machining of Perspex.

The hypothesis under test is that modifications to the container geometry result in mode structures that can still be described by combinations of the mode structures for simpler geometries. Attention is restricted to the case where the modifications are simple, meaning that (as with the chosen baffles) they are made up of shapes based on a right circular axisymmetric geometry. Specifically, the following was conjectured:

1) With the largest r/R of 0.777, and the system forced near the (1, 1, 1) resonance for the original tank, the behavior would be essentially that of the (1, 1, 1) mode.

2) With the smallest r/R of 0.222, it was predicted that two separate contained flows would develop, one in the upper and one in the lower half-cylinder. It was expected that the mode structure observed would be that of the (1, 2, 1) mode as given in Table 2, which occurs at almost the same frequency as the (1, 1, 1) resonance in the original tank.

3) For the intermediate baffle with $r/R = 0.622$, it was conjectured that a low-order mode structure would not be identified and that this baffle would therefore be "optimal" for the mode tank.

IV. Experimental Apparatus and Procedure

A schematic diagram of the apparatus is given in Fig. 1.

The Perspex tank has an internal diameter of 90 mm and internal height of 120 mm. It spins in a gimbal frame that is in turn mounted on a turntable. Thus ω_1 is the spin rate of the tank in the gimbal frame, and the precessing rate ω_2 is the turntable speed. The nutation angle θ can be varied by tilting the gimbal frame from the vertical. The tank spin axis is precessed at constant θ. This nutation angle can be preset at a desired value, and precession can be initiated by an impulsive tilt of the gimbal frame to the preset value.

Table 2 Eigenfrequencies for each half of a sectioned cylinder: the baffle insert gives the lower cylinder a slightly different aspect ratio

Upper cylinder, aspect ratio 1.333				Lower cylinder, aspect ratio 1.349			
k	l	ω_{kl1}	λ_{kl1}	k	l	ω_{kl1}	λ_{kl1}
1	1	1.48403	2.58361	1	1	1.49458	2.58706
1	2	2.65373	5.79179	1	2	2.68187	5.79590
1	3	3.93394	8.96467	1	3	3.97849	8.96888
2	1	1.12768	2.45622	2	1	1.13061	2.45735
2	2	1.55602	5.61787	2	2	1.56698	5.61973
2	3	2.11440	8.77909	2	3	2.13391	8.78121
3	1	1.05736	2.42832	3	1	1.05869	2.42886
3	2	1.27305	5.56885	3	2	1.27883	5.56987
3	3	1.58811	8.72080	3	3	1.59943	8.72207
4	1	1.03239	2.41818	4	1	1.03314	2.41848
4	2	1.16044	5.54891	4	2	1.16396	5.54953
4	3	1.36056	8.69507	4	3	1.36792	8.69590

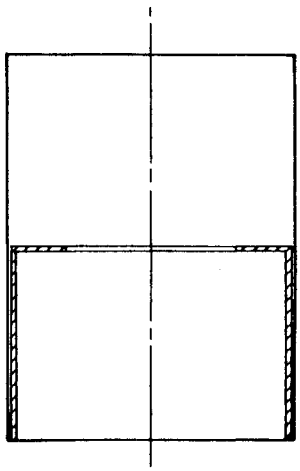

Fig. 2 Baffle fitted in tank. Shown here is the baffle with $r/R = 0.622$; other baffles had $r/R = 0.777$ and 0.222.

Flow inside the tank was illuminated by a sheet of white light and was viewed by a video camera from the turntable frame of reference, from where still photographs were taken simultaneously. The flowfield inside the tank was visualized by the introduction of pearlescent flakes. It can be assumed[11] that these highly reflective flakes are aligned at a particular inclination to the strain field in the fluid. The pearlescence technique should be regarded as an essentially qualitative technique. It gives a picture of the structure of the flow but no information about the magnitudes of strain or velocity. The tank was completely filled with water.

A baffle assembly is shown in Fig. 2. The baffles are inserts that fit tightly inside the tanks but are not rigidly fixed so that they can be readily exchanged. The wall thickness of the inserts is of the order of the boundary-layer thickness, which scales[2] as $E^{1/4}$. Note from Table 2 that the lower cylinder has a slightly different aspect ratio due to the presence of the insert wall. They were fitted within the tank to a tolerance of ± 0.2 mm. From Table 2, the difference in aspect ratios causes only a slight (1%) shift in the eigenfrequency spectrum. None of the flows observed with the baffles in place showed a systematic difference in behavior above and below the baffle. Thus it was concluded that the change in diameter in the lower half due to the presence of the insert wall had a negligible influence on the flow behavior.

An inviscid interior solution based on a free-slip boundary condition had been shown[10] to give a good qualitative description of the mode structures. If the baffles underwent an azimuthal slipping motion relative to the tank walls, the inviscid interior flow would not be affected. Thus it was felt that it was not important if the baffle inserts were not fixed rigidly to the tank walls. Net vertical flows that might have lifted the baffle plate from the horizontal centerline were not expected from the flows that had been observed previously.[10] No vertical motion of the baffle insert could be discerned during experiments.

V. Experiments Results and Discussion

The behavior during spin up with each baffle in the tank is interesting. In the original tank without baffles, a bright column can be seen shrinking inward to the tank axis.[10] Now with the baffles in the tank, the shrinking bright column exhibits a transient axial waviness of indeterminate wave number and appears to pulsate as it shrinks. As in the original tank, this bright column never completely vanishes. Its radial extent will be used to define a core region in the visualized pattern. Experiments conducted by the author in the original tank using a thymol blue visualization technique[12] had con-

firmed that the fluid was not in solid-body rotation. This was suspected to be caused by irregularities in the spin rate and geometry of the tank. The relative velocity of the departure from solid-body rotation was estimated as being of order 10^{-3} and its sign was opposite to that of ω_1. It was not expected to influence the development of eigenmodes; in Manasseh[9] it was shown to be two orders of magnitude smaller than the amplitude of the forced motion.

A. Experiments with $r/R = 0.777$ Baffle

With the $r/R = 0.777$ baffle, the system was run to excite what would have been the (1, 1, 1) mode in the original right cylinder of aspect ratio 2.666. The nutation angle θ was 1 deg. It had been expected that the behavior for this r/R ratio would approximate that of the (1, 1, 1) mode in the original tank. However, three axial half-wavelengths were consistently observed rather than one, indicating that a $k = 3$ mode was being excited. Figure 3 shows this state. An eigenfrequency spectrum is presented in Table 3 for the cylindrical region inside the baffle, which has an aspect ratio of 3.428. Clearly there are a number of $k = 3$ modes that could be excited at an ω of about 2.6 ($\omega_2 = 30$ rpm for $\omega_1 = 100$ rpm). If this is indeed the case, an effective boundary condition $\boldsymbol{u} \cdot \hat{\boldsymbol{n}} = 0$ would be required at the inner radius of the baffle, where $\hat{\boldsymbol{n}}$ is the normal to the boundary of the cylindrical region inside the baffle. However, there is no physical barrier to provide such a boundary condition throughout the tank height.

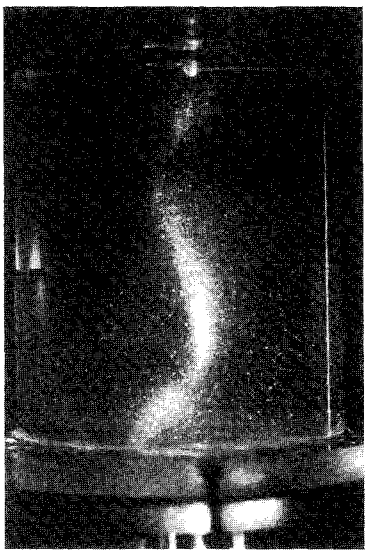

Fig. 3 Experiment with baffle $r/R = 0.777$: $\omega = 2.6$ ($\omega_2 = 30$ rpm, $\omega_1 = 100$ rpm), $\theta = 1$ deg.

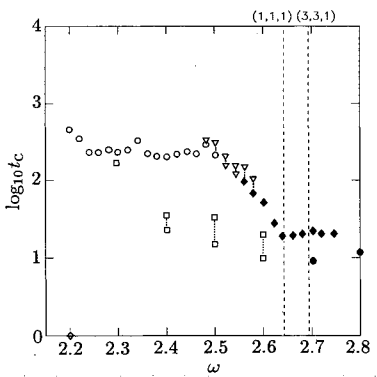

Fig. 4 Breakdown times with a baffle of $r/R = 0.777$, and in the original unbaffled tank. Nutation angle $\theta = 1$ deg, $\omega = 2(1 + \omega_2/\omega_1)$, $\omega_1 = 100$ rpm; t_c = number of revolutions of tank relative to turntable before breakdown; □: breakdown of type E nature; ●: breakdown of type A nature in baffled tank; ◇ on ω axis: no breakdown during the 200 revolutions for which experiment was run in baffled tank; ○: instabilities thought to be due to thermal effects in unbaffled tank; ▽: type C breakdown in unbaffled tank; ◆: type A breakdown in unbaffled tank.

Table 3 Eigenfrequencies for a cylinder of aspect ratio 3.428

k	l	m	ω_{klm}	λ_{klm}	k	l	m	ω_{klm}	λ_{klm}
1	1	0	4.29963	3.83171	2	2	2	4.29329	7.65146
1	2	0	7.72146	7.01557	3	1	2	1.81470	4.16270
2	1	0	2.31769	3.83170	3	2	2	2.88779	7.44709
2	2	0	3.95665	7.01554	1	1	3	6.70788	6.07773
3	1	0	1.71551	3.83170	1	2	3	10.3730	9.46050
3	2	0	2.74107	7.01558	2	1	3	3.32774	5.81654
1	1	1	3.44696	3.02260	2	2	3	5.11942	9.20111
1	2	1	6.88198	6.23901	3	1	3	2.27652	5.62184
2	1	1	1.76748	2.67081	3	2	3	3.42457	9.00350
2	2	1	3.36624	5.89047	1	1	4	8.09467	7.36032
3	1	1	1.36215	2.54247	1	2	4	11.8696	10.8374
3	2	1	2.31555	5.74104	2	1	4	4.02820	7.15098
1	1	2	5.21500	4.68982	2	2	4	5.88550	10.6289
1	2	2	8.76351	7.97753	3	1	4	2.72797	6.97689
2	1	2	2.58048	4.35945	3	2	4	3.93205	10.4534

However, the most important feature of this experiment is the very rapid breakdown of the flow, which appears similar in nature to the breakdowns described in Manasseh.[10] The structure with three axial half-wavelengths never appears to be stable or even to grow monotonically. Comparison is made in Fig. 4 with the breakdown times of the (1, 1, 1) mode in a tank without baffles. The symbols □, •, and ◇ are for the experiment with the baffle and the symbols ▽, ◆, and ○ are for the experiment without the baffle. A ○ symbol for the unbaffled case denotes "nonbreakdown" event, where the flow exhibited only weak long-time-scale instabilities thought to be due[10] to spurious thermal effects. A • symbol for the baffle case (◆ for the unbaffled case) denotes a breakdown regime where fine-grain turbulence is generated. Where (for the baffle case) there are two square symbols at the same ω, the breakdown is reminiscent of the type E breakdown regime[10] in the original tank. Here turbulence develops rapidly in the core region, then spreads to the tank walls after a discernible pause; this time is indicated by the second square type E symbol in Fig. 4. Characteristic lines can be seen emanating from the baffle inner radius. The introduction of this baffle has significantly decreased breakdown times. Experiments done with this baffle at a nutation angle of 3 deg resulted in a reduction of the breakdown time to about 60% of the breakdown time of the (1, 1, 1) mode. The breakdown types identified by the symbols in Fig. 4 are those defined by Manasseh.[10]

With the $r/R = 0.777$ baffle in the tank, the system was also run at a range of ω, from 1.2 to 1.4 ($\omega_2 = -40$ to -30 rpm for $\omega_1 = 100$ rpm) that would have excited the (3, 1, 1) mode in a tank without baffles. The nutation angle θ was 3 deg. In this ω range the presence of the $r/R = 0.777$ baffle again gives faster breakdown times.

B. Experiments with $r/R = 0.222$ Baffle

The baffle with the smallest hole could similarly support a range of modes in a hypothetical cylinder of aspect ratio 12.0. These are tabulated in Table 4, where it can be seen that there are no obvious low-order modes that would be excited in the ω range tested. Once again the system was forced with a range of frequencies that would have excited the (1, 1, 1) mode in a tank without baffles. Two nutation angles were tested, $\theta = 1$ and 3 deg. The flow observed here is strongly columnar with complex organization within a cylinder that passes through the hole and little apparent activity in the rest of the tank. A wavy axial structure is seen in this "inner cylinder" and can be interpreted as evidence of modal behavior. Figure 5 shows this state. It cannot be said if it is a mode appropriate to the cylinder of aspect ratio 12.0, or a combination of the (1, 2, 1) modes for the two half-cylinders of aspect ratio 1.3, or both.

Table 4 Eigenfrequencies for a cylinder of aspect ratio 12.0

k	l	m	ω_{klm}	λ_{klm}	k	l	m	ω_{klm}	λ_{klm}
1	1	0	14.6701	3.83170	2	2	2	15.6115	8.15739
1	2	0	26.8162	7.01559	3	1	2	6.12847	4.74878
2	1	0	7.38601	3.83169	3	2	2	10.2795	8.03521
2	2	0	13.4360	7.01558	1	1	3	24.0565	6.29253
3	1	0	4.98012	3.83171	1	2	3	36.9639	9.67359
3	2	0	8.98831	7.01557	2	1	3	11.8931	6.20517
1	1	1	13.6604	3.56670	2	2	3	18.3366	9.58676
1	2	1	25.8207	6.75479	3	1	3	7.85551	6.11951
2	1	1	6.41499	3.31782	3	2	3	12.1394	9.50185
2	2	1	12.4865	6.51693	1	1	4	28.7520	7.52271
3	1	1	4.08314	3.10923	1	2	4	42.0256	10.9991
3	2	1	8.10959	6.32065	2	1	4	14.2771	7.45715
1	1	2	19.1393	5.00382	2	2	4	20.9060	10.9338
1	2	2	31.6663	8.28608	3	1	4	9.46513	7.39229
2	1	2	9.36105	4.87338	3	2	4	13.8752	10.8692

Table 5 Eigenfrequencies for a cylinder of aspect ratio 4.287

k	l	m	ω_{klm}	λ_{klm}	k	l	m	ω_{klm}	λ_{klm}
1	1	0	5.32193	3.83169	2	2	2	5.39023	7.76531
1	2	0	9.62262	7.01555	3	1	2	2.18297	4.26729
2	1	0	2.79835	3.83170	3	2	2	3.57914	7.55750
2	2	0	4.88862	7.01555	1	1	3	8.43076	6.13644
3	1	0	2.00895	3.83170	1	2	3	13.0236	9.51862
3	2	0	3.34322	7.01554	2	1	3	4.15569	5.91354
1	1	1	4.40827	3.14719	2	2	3	6.42031	9.29779
1	2	1	8.72867	6.35632	3	1	3	2.79113	5.73056
2	1	1	2.13739	2.76946	3	2	3	4.26361	9.11463
2	2	1	4.20858	5.99340	1	1	4	10.1514	7.40518
3	1	1	1.55022	2.60499	1	2	4	14.8788	10.8820
3	2	1	2.82784	5.81693	2	1	4	5.03264	7.23111
1	1	2	6.58766	4.77304	2	2	4	7.37259	10.7088
1	2	2	11.0393	8.05897	3	1	4	3.36975	7.07665
2	1	2	3.21110	4.47361	3	2	4	4.90244	10.5543

In Fig. 6, the breakdown behavior is summarized for tests with this baffle at both $\theta = 3$ deg (• and □ symbols) and at $\theta = 1$ deg (◇ and △ symbols). At $\theta = 1$ deg, no breakdowns could be discerned until about $\omega = 2.5$ ($\omega_2 = 25$ rpm for $\omega_1 = 100$ rpm). Results for $r/R = 0.622$ baffle are also in this figure and will be discussed shortly. The complex wavy structure persists for over 200 revolutions. The breakdowns that did occur were weak; they did not generate fine-grain turbulence. Triangles denote these breakdowns.

For tests done with the nutation angle at 3 deg, the flow does break down over a wider frequency range. Where there is a • and a □ symbol at the same ω, the • symbol indicates when fine-grain turbulence is generated and is confined within the baffle inner radius. This first breakdown occurs in only about 50% of the breakdown time for the (1, 1, 1) mode in the original tank. The □ symbol indicates a discernible pause before the flow in the entire tank becomes disordered.

C. Experiments with $r/R = 0.622$ Baffle

With the intermediate baffle and the system forced at $\theta = 1$ deg there is no clear modal structure. The core flow develops an axial waviness of indeterminate wave number and very small radial extent. This state is shown in Fig. 7. Characteristics can again be observed emanating from the inner radius of the baffle. If $\omega = 2.36$ ($\omega_2 = 18$ rpm for $\omega_1 = 100$ rpm), the characteristics of the system are at an angle $\alpha = 25$ deg to the tank axis and a perfect double cone fits in the hole in the baffle, forming a diamond pattern. One or two sides of this diamond can be faintly seen in Fig. 7. An examination of the eigenfrequencies in Table 5 for a hypothetical cylinder of aspect ratio 4.287 shows that there are no obvious low-order modes that would be forced at the ω range tested. In Fig. 6 the breakdown behavior is summarized for tests with the intermediate baffle at both $\theta = 3$ (◆ symbols) and 1 deg (○ and ▲

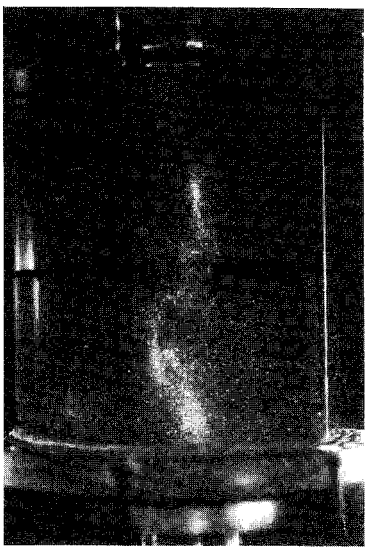

Fig. 5 Experiment with baffle $r/R = 0.222$: $\omega = 2.6$ ($\omega_2 = 30$ rpm, $\omega_1 = 100$ rpm), $\theta = 1$ deg.

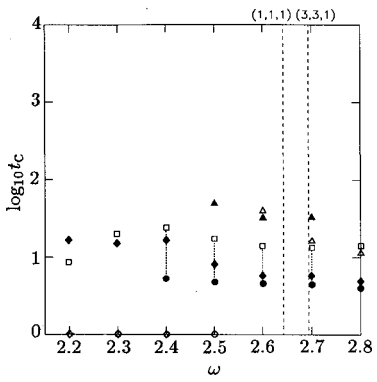

Fig. 6 Breakdown times with baffle $r/R = 0.222$ and 0.622: $\omega = 2(1 + \omega_2/\omega_1)$, $\omega_1 = 100$ rpm, t_c = number of revolutions of tank relative to turntable before breakdown; • and □: $\theta = 3$ deg, $r/R = 0.222$; △ and ◇: $\theta = 1$ deg, $r/R = 0.222$; ◇ on ω axis: no breakdown during the 200 revolutions for which the experiment was run, $r/R = 0.222$; ◆: $\theta = 3$ deg, $r/R = 0.622$; ▲ and ○: $\theta = 1$ deg, $r/R = 0.622$; ○ on ω axis: no breakdown during the 200 revolutions for which the experiment was run, $r/R = 0.622$.

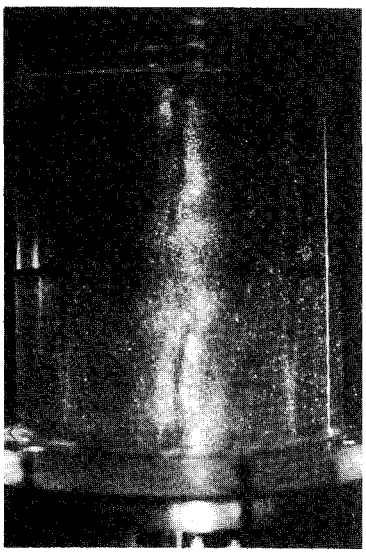

Fig. 7 Experiment with baffle $r/R = 0.622$: $\omega = 2.5$ ($\omega_2 = 25$ rpm, $\omega_1 = 100$ rpm), $\theta = 1$ deg.

symbols). Disordering of this flow with $\theta = 1$ deg does not occur until about $\omega = 2.6$ ($\omega_2 = 30$ rpm for $\omega_1 = 100$ rpm). Weak flow breakdowns or disorderings at higher frequencies are denoted by ▲ symbols.

For tests done with $\theta = 3$ deg, a modal structure briefly appears, apparently with three axial half-wavelengths. The flow breaks down over all of the frequency ranges investigated. Fine-grain turbulence is generated at the baffle inner radius, and the whole flow rapidly becomes disordered in about 40% of the breakdown time of the (1, 1, 1) mode.

D. Discussion

With hindsight, the apparent preference for flow structures organized in vertical columns might be expected. Slowly varying or "quasigeostrophic" flows in rotating systems can be shown[2] to have small vertical variation in their flowfields. Any columnar flow based on the baffle inner radius is thus a solution of the steady unforced equations of motion, and its presence could allow the extension of the vertical boundary layer on the inner rim of the baffle throughout the height of the tank. Such an internal shear layer may partition the tank into an "annulus" and an "inner cylinder" in which inertial modes are confined. A shear layer does not, in general, behave as a rigid boundary that supports an oscillating pressure field. However, it is conceivable that the reduction in the fluid's angular velocity across the shear layer is sufficient such that, in the annulus, the frequency is "Doppler-shifted" to make $|\omega| < 1$. From Eq. (6), it can be seen that wave propagation is no longer possible when $|\omega| < 1$. The propagation of waves would then be confined to the inner cylinder.

The reduction in breakdown times supports the notion that the modifications to the geometry may generate waves that rapidly destroy any modal structure. Here we would assume that as an ordered modal flow develops, it impinges on the baffles and generates plane wave. Reflected plane waves interact with each other and the ordered modal flow, rapidly disordering the flow.

VI. Conclusions

1) The specific predictions 1) and 2) given in Sec. III of the hypothesis under test have been refuted. They were based on the assumption that modal behavior would be generated in the two half-height cylinders formed by the baffle sectioning the original cylinder in two. However, it appears that a modal description may still be valid if the volume generating the mode is taken as a single cylinder bounded by the baffle inner radius. In the case of the baffle with the largest hole, a modal description based on such an inner cylinder with a hypothetical rigid wall may be briefly valid. Similarly, there is evidence of modal behavior for the baffle with the smallest hole. However, the geometrical origin of this mode is uncertain; Table 4 shows that there are no low-order modes particularly close to resonance in a hypothetical cylinder of aspect ratio 12.0.

For the intermediate baffle shape a modal description appears to be only briefly valid when the system is forced strongly ($\theta = 3$ deg). It was predicted (prediction in Sec. III) that no modal structure would be found because it was thought that the baffle would act as a sharp "obstacle" precluding the development of the (1, 1, 1) mode in the original cylinder. This prediction has not been refuted. There is some evidence of axial waviness; nevertheless, it appears that the development of a low-order mode has been successfully forestalled.

2) The modes that develop in the case of the baffle with the largest hole do not survive over time scales similar to the modes in the original geometry. They break down significantly faster than in the original tank, for all of the cases tested. For the baffles with the smallest and intermediate-sized holes, the behavior is more complicated. At $\theta = 1$ deg, flow breakdowns are nonexistent or weak, but at $\theta = 3$ deg, fine-grain turbulence is rapidly generated at the baffle inner radius.

3) In the engineering context, any modes that do briefly develop may still cause undesirable instabilities of the spacecraft. At a nutation angle of $\theta = 1$ deg, modes were observed for the baffles with the largest and smallest holes. Further experiments may help elucidate the mechanism(s) by which these structures are generated. For example, it would be interesting to test experimentally for the presence of a shear layer at the baffle inner radius that forces wave activity to be confined to the region inside the baffle.

4) For a given excitation frequency and small nutation angle, a simple baffle configuration has been found that precludes the development of modal behavior in a right cylindrical tank. If modal flow behavior is deemed to be undesirable from the spacecraft dynamics point of view, then the identification of such optimum baffles is an obvious objective. Use of the simple flow visualization technique employed here is suggested as an adjunct to existing spacecraft test programs.

Direct comparisons of the drop-test experiments reported by Pocha[1] with the experiments reported in this paper are probably unwise, as the geometry of the drop-test tanks was not a simple right circular cylinder and the fluid dynamics and rigid container dynamics were fully coupled in the drop tests. Nevertheless, the existence in the drop tests of an optimal radius ratio with a clear maximum in the time constant for instability supports the contention that fluid modal behavior is involved in the instability and that the optimal baffle has tuned the tank away from a destabilizing resonance.

Acknowledgments

This work was done as part of a project funded by the British National Space Centre/Royal Aerospace Establishment under Contract D/ER1/9/4/2029/206/SP(F) and managed by British Aerospace PLC. I should like to acknowledge the support of those organizations. I did this work while a graduate student in the Department of Applied Mathematics and Theoretical Physics (DAMTP), University of Cambridge. I owe thanks to my supervisor, Paul Linden, as well as to my colleagues, in particular David Tan, Michael McIntyre, and John Jackson, for many helpful discussions. The apparatus was constructed by DAMTP technicians.

References

[1]Pocha, J. J., "An Experimental Investigation of Spacecraft Sloshing," *Space Communications and Broadcasting,* Vol. 5, No. 4, 1987, pp. 323–332.

[2]Greenspan, H. P., *The Theory of Rotating Fluids,* Cambridge Univ. Press, Cambridge, England, UK, 1968.

[3]Wood, W. W., "An Oscillatory Disturbance of Rigidly Rotating Fluid," *Proceedings of the Royal Society of London, Series A: Mathematical and Physical Sciences,* Vol. 293, 1966, pp. 181–212.

[4]Kelvin, Lord, "Vibrations of a Columnar Vortex," *Philosophical Magazine,* Vol. 10, 1880, pp. 155–168.

[5]Scott, W. E., "The Large Amplitude Motion of a Liquid-Filled Gyroscope and the Non-Interaction of Inertial and Rossby Waves," *Journal of Fluid Mechanics,* Vol. 72, 1975, pp. 649–660.

[6]Whiting, R. D., "An Experimental Study of Forced Asymmetric Oscillations in a Rotating Liquid Filled Cylinder," Ballistic Research Labs, Rept. ARBRL-TR-02376, Aberdeen Proving Ground, MD, Oct. 1981.

[7]Malkus, W. V. R., "Precession of the Earth as the Cause of Geomagnetism," *Science,* Vol. 160, April 1968, pp. 259–264.

[8]McEwan, A. D., "Inertial Oscillations in a Rotating Fluid Cylinder," *Journal of Fluid Mechanics,* Vol. 40, 1970, pp. 603–640.

[9]Manasseh, R., "Inertia Wave Breakdown: Experiments in a Precessing Cylinder," Ph.D. Thesis, Univ. of Cambridge, Cambridge, England, UK, 1991.

[10]Manasseh, R., "Breakdown Regimes of Inertia Waves in a Precessing Cylinder," *Journal of Fluid Mechanics*, Vol. 243, 1992, pp. 261–296.

[11]Savas, S., "On Flow Visualization Using Reflective Flakes," *Journal of Fluid Mechanics,* Vol. 152, 1985, pp. 235–248.

[12]Baker, J. D., "A Technique for the Precise Measurement of Small Fluid Velocities," *Journal of Fluid Mechanics,* Vol. 26, 1966, pp. 573–575.